



Evaluation of Lime Juice as Potential Green Corrosion Inhibitor Using Gravimetric and Electrochemical Studies

S.J. HEPZIBA MAGIE JESSIMA^{1,*}, B.G. RAKESH¹, MOKSHA MUTHAPPA¹ and S. SUBHASHINI²

¹Department of Chemistry, CHRIST (Deemed to be University), Bengaluru-560029, India

²Department of Chemistry, Avinashilingam Institute for Home Science and Higher Education for Women (Deemed to be University), Coimbatore-641043, India

*Corresponding author: E-mail: hepziba.magie@christuniversity.in

Received: 20 March 2020;

Accepted: 29 May 2020;

Published online: 27 July 2020;

AJC-19990

Lime, a vibrant fruit of citrus family is known for its antioxidant as well as anti-microbial properties. The constituents of lime juice include organic acids, polyphenols, soluble sugars, vitamins, minerals and amino acids. These details prompted to experiment lime juice as corrosion inhibitor for mild steel in 1 M HCl. The weight loss studies showed that the corrosion inhibition efficiency increased with increase in concentration of the lime juice as well as increase of temperature. The inhibition efficiency reached a maximum of 96% for an immersion period of 24 h. The best fit for the adsorption process obeyed Langmuir isotherm. The negative value of ΔG_{ads} showed the spontaneity of the corrosion inhibition process. The corrosion inhibition efficiency of the acidified lime juice was further validated by electrochemical studies namely AC impedance studies and potentiodynamic polarization studies. The surface morphology study was performed used optical profilometer.

Keywords: Mild steel, Corrosion inhibitor, Lime, Green inhibitor, Optical profilometer.

INTRODUCTION

Metals have a natural tendency to find all the possible routes to go back to their stable combined state. This results in the gradual destruction of the metals which is referred as corrosion. Chemical cleaning of the industrial equipment employs acids such as hydrochloric acid, sulphuric acid, nitric acid and phosphoric acid so as to remove the scales, rust or inorganic contaminants. However, hydrogen from the acid reacts with the metal surface making it brittle and causes cracks. The use of corrosion inhibitors in corrosive environments to mitigate corrosion was found to be an effective method in terms of availability, cost effectiveness and ease of application [1]. The organic and inorganic inhibitors are known for their effective performance as inhibitors for mild steel due to the presence of the hetero atoms and ability to be adsorbed onto the surface of the metal preventing its corrosion. Yet the high cost, toxicity, non-biodegradability and the great threat they pose to the environment led to the search for environmentally friendly inhibitors. Naturally occurring plant materials which have the constituents

and properties similar to that of the synthetic materials are exploited in the mitigation of corrosion. Several studies have showed the use of fruit juices as effective corrosion inhibitor [2-11]. Lime juice is rich source of flavonoids [12], polyphenols [13,14], minerals [15], organic acids [16], sugars [17] and fatty acids [18]. Studies also revealed the phytochemical antioxidant and antimicrobial properties of lime juice [19]. The objective of the present study was to evaluate lime juice as an effective corrosion inhibitor of mild steel in 1 M HCl using weight loss study and electrochemical studies.

EXPERIMENTAL

Fully ripened lime purchased from the local market was washed with tap water, dried and then compressed using lemon hand juicer. About 22 mL juice was obtained from 35 g of lime. The juice was filtered to get a homogeneous solution and the fresh juice was used for all the experiments. After testing a range of concentrations, 8 to 18% concentrations (v/v) of lime juice with 1 M HCl was chosen for testing the inhibitor activity. The mild steel specimen of dimension 1 cm × 5 cm was mechan-

ically polished followed by the use of emery sheets. Then washed with distilled water, degreased with acetone, dried and stored in the desiccator until further use. For weight loss studies, accurately weighed mild steel specimens are placed in 100 mL beakers containing 1 M HCl without and with varying % composition of lime juice extract. After an immersion periods of 1, 3, 6, 12 and 24 h, the weight loss of the mild steel specimens were accurately measured. The experiment was repeated at different temperatures *viz.* 303-343 K through a step up of 10 °C raise in temperature. Using the weight loss values, the inhibition efficiency % and surface coverage at different immersion periods were calculated using eqns. 1 and 2.

$$IE (\%) = \left(\frac{W_b - W_i}{W_b} \right) \times 100 \quad (1)$$

$$\text{Surface coverage } (\theta) = \frac{IE\%}{100} \quad (2)$$

where W_b and W_i represent the weight loss in g for the blank and the inhibitor solution, respectively. The electrochemical studies were done using CH Electrochemical workstation CHI-608E model constituting three electrode cell system with platinum as counter electrode, calomel as reference electrode and mild steel specimen of 1 cm × 1 cm dimension as working electrode. Both AC impedance and Tafel polarization studies were performed. The surface morphology was studied using optical profilometer.

RESULTS AND DISCUSSION

Weight loss studies: Weight loss studies showed that the inhibition efficiency of the corrosion inhibitor namely the lime juice increased with the increase in concentration as well as increase in immersion periods as shown in Fig. 1. The inhibition efficiency reached 96% for an immersion period of 24 h. An increase in inhibition efficiency with increase in concentration may be attributed to the increase in the concentration of the active constituents being adsorbed on the surface of the metal [20]. The temperature studies revealed that the corrosion inhibition efficiency increases with increase in temperature and reaches a maximum of 94.59% at 343 K for 18% inhibitor concentration and an immersion period of 30 min as shown in Fig. 2. The corrosion rate was calculated using eqn. 3.

$$\text{Corrosion rate (mpy)} = \frac{3.45 \times 10^6 \times \Delta w}{(A \times d \times t)} \quad (3)$$

Conc. (v/v)	Corrosion rate (mpy)				
	303 K	313 K	323 K	333 K	343 K
Blank	613.1646	1716.861	2505.215	4362.228	11650.13
8%	262.7848	630.6835	875.9494	1331.443	2803.038
10%	210.2278	508.0506	718.2785	1208.81	2102.278
12%	157.6709	402.9367	508.0506	875.9494	1576.709
14%	122.6329	297.8228	385.4177	630.6835	1313.924
16%	70.07595	175.1899	245.2658	367.8987	893.4684
18%	52.55696	122.6329	175.1899	262.7848	630.6835

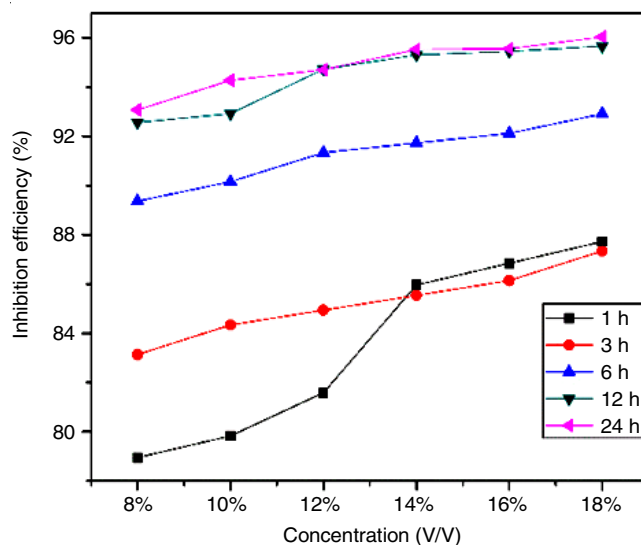


Fig. 1. Variation of IE% with lime juice concentrations in 1M HCl for mild steel at different immersion periods at 303 K

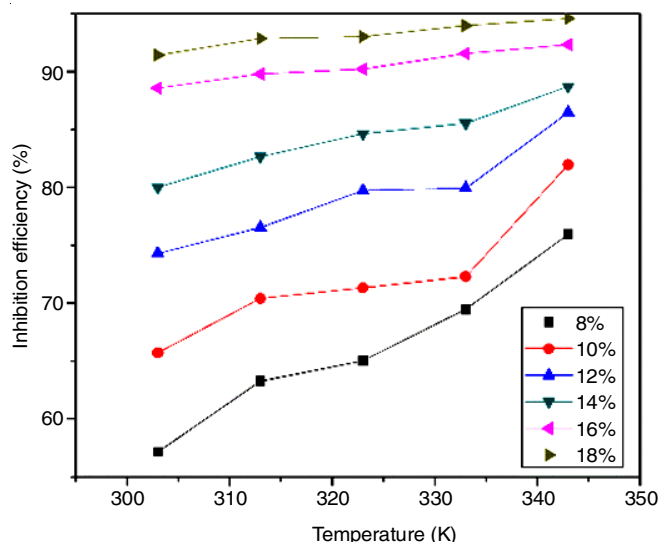


Fig. 2. Variation of IE% with concentrations of lime juice in 1M HCl for mild steel at different temperatures

where ΔW is the weight loss before and after immersion of the mild steel specimen in the blank and the inhibitor solutions, A is the area of the specimen, t is the immersion period and d is the density of the mild steel. It is clearly seen from Table-1 that the corrosion rate decreases with the increase in concentration of the inhibitor solutions.

The Arrhenius plot (Fig. 3) and transition state plot (Fig. 4) were drawn based on eqns. 4 and 5. These plots were useful to calculate the corrosion kinetic parameters and the values are displayed in Table-2.

$$CR = A \exp\left(\frac{E_a}{RT}\right) \quad (4)$$

$$CR = \frac{RT}{Nh} \exp\left(\frac{\Delta S^\ddagger}{R}\right) \exp\left(\frac{-\Delta H^\ddagger}{RT}\right) \quad (5)$$

where CR is the corrosion rate, E_a is the apparent activation energy, A is the pre exponential factor and R is the molar gas

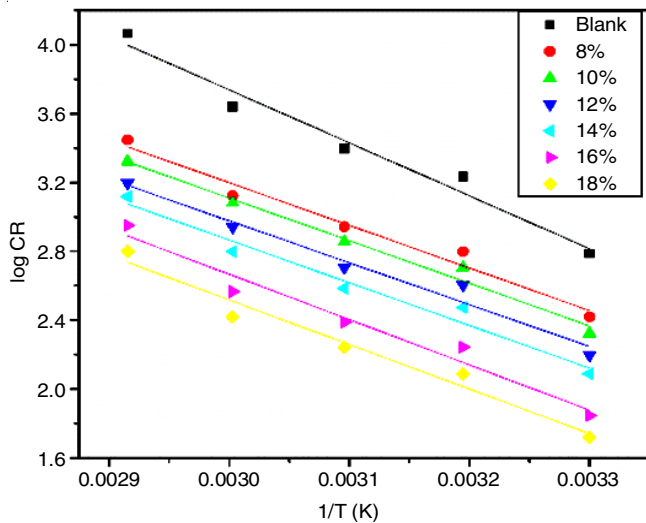


Fig. 3. Arrhenius plot for mild steel in the absence and presence of lime juice in 1M HCl

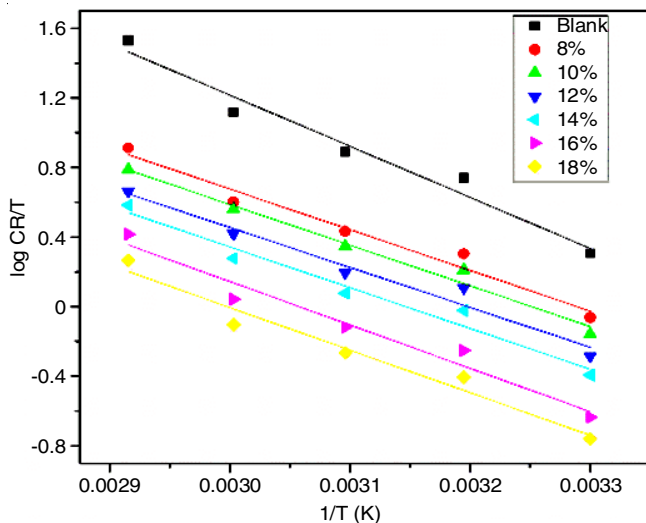


Fig. 4. Transition state equation plot for mild steel in the absence and presence of lime juice in 1M HCl

Conc. (v/v)	E _a (kJ mol ⁻¹)	A (kg m ⁻² s ⁻¹)	ΔH [*] (kJ mol ⁻¹)	ΔS [*] (J mol ⁻¹ K ⁻¹)	E _a -ΔH = RT
Blank	58.90	9.26×10 ¹²	56	-5.64	2.68
8%	47.39	4.20×10 ¹⁰	44.7	-50.49	2.68
10%	47.39	3.42×10 ¹⁰	44.7	-52.19	2.68
12%	46.59	1.89×10 ¹⁰	43.9	-57.14	2.68
14%	47.47	2.01×10 ¹⁰	44.8	-56.63	2.68
16%	50.38	3.63×10 ¹⁰	47.7	-51.71	2.68
18%	49.48	1.86×10 ¹⁰	46.8	-57.26	2.68

constant, T is the temperature in K. From Table-2, it is clear that E_a values for the inhibited solution is lower than that of the uninhibited solution. This implies the formation of a chemisorbed layer of the inhibitor that helps in decreasing the metal dissolution process [21]. An increase in inhibition efficiency with the increase in temperature further support the chemisorption process. The positive values of enthalpy of activation

ΔH^{*} values reflect the endothermic nature of the corrosion process. The large and the negative value of entropy of activation suggests a greater orderliness due to the formation of activated complex [22].

The inhibitory action of the inhibitor in acid solution is mainly due to the adsorption on the surface of the metal. Also, an inhibitor molecule may occupy more than one active site on the surface or else more than one inhibitor molecule may adsorb on an active site leading to a multilayer adsorption [23]. The adsorption studies showed that the adsorption process obeyed Langmuir, Temkin and Freundlich isotherms as was established by the R² value. However, the best fit was found for Langmuir isotherm. The deviation of the slope from unity implies the possible interactions between the adsorbed molecules causing repulsions or attractions or may be due to the changes in heat of adsorption with increase in surface coverage [24]. Therefore, the results were once again fitted in the modified form of Langmuir isotherm given by eqn. 6:

$$\log\left(\frac{\theta}{1-\theta}\right) = \log K + y \log C \quad (6)$$

where y refers to the number of inhibitor molecules adsorbed on an active site. The value of 1/y calculated was found to be less than 1 indicating a multilayer adsorption [23,25]. An increase in K_{ads} values with temperature reveals the increased stability of the adsorbed inhibitor on the metal surface (Table-3). This is further evident from the increase in the inhibition efficiency with increase in temperature [26].

Temp. (K)	K _{ads}	ΔG _{ads} (KJ mol ⁻¹)	Slope	R ²
303	0.057	-2.89	0.55	0.99
313	0.086	-4.07	0.65	0.99
323	0.099	-4.57	0.68	1.00
333	0.117	-5.17	0.72	0.98
343	0.231	-7.28	0.85	1.00

Electrochemical studies: The kinetics of the corrosion process and the effectiveness of the inhibition can be established with the help of electrochemical methods. Nyquist plot, Bodes and phase angle plots obtained for mild steel in absence and in presence of the inhibitor of varying concentrations at 303 K are shown in Figs. 5 and 6. The diameter of semi-circle extrapolated in the Nyquist plot gives the charge transfer resistance equivalent to the polarization resistance R_p. The increase in diameter with the inhibitor concentration may be attributed to the increased resistance against the metal dissolution by the adsorbed inhibitor molecules at the metal solution interface [27]. These adsorbed molecules block the transfer of electrons from the metal surface to the solution. The presence of single semi-circle loop in Nyquist plot and single maxima in Bodes plot indicates both the corrosion process and the inhibition is controlled by charge transfer phenomenon [28]. The phase angle plot reveals lesser than -90° phase angle at all inhibitor concentration that can be corroborated to non-ideal capacitor [29].

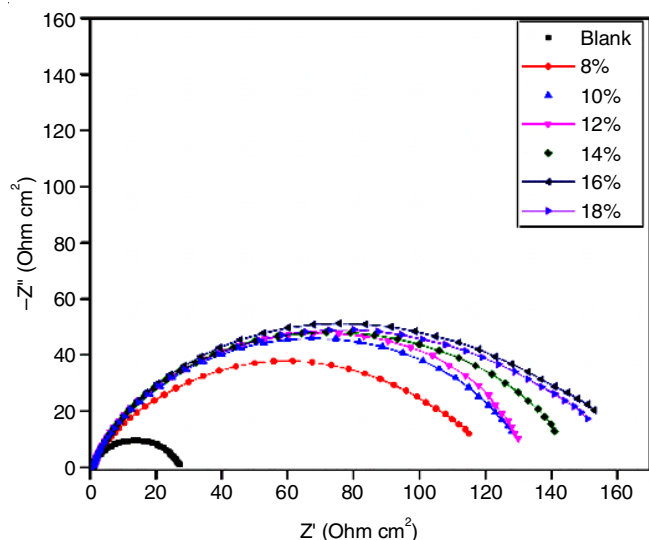


Fig. 5. Nyquist plot for mild steel in the absence and presence of lime juice of different concentrations in 1M HCl

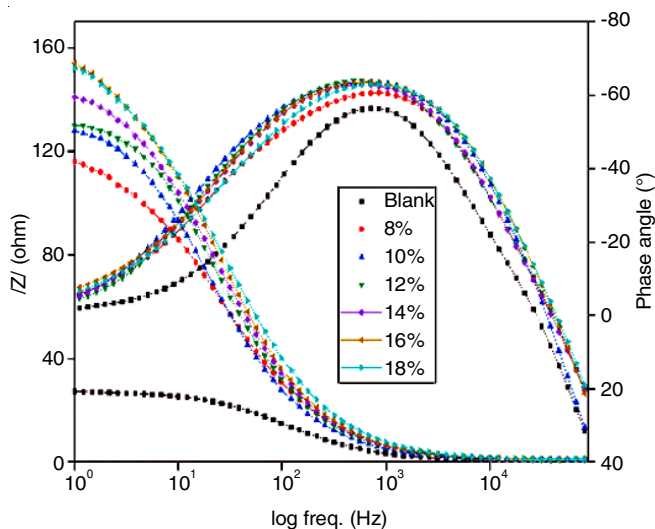


Fig. 6. Bodes and phase angle plots for mild steel in the absence and presence of lime juice in 1M HCl

The experimental data was fitted with an equivalent circuit displayed in Fig. 7. The electrochemical impedance parameters namely solution resistance (R_s), constant phase element (CPE) values, polarization resistance (R_p) and the corrosion inhibition efficiency calculated from R_p are listed in Table-4. From Fig. 5, it is clear that all the semi-circles are depressed at the center towards the real axis due to the frequency dispersion, surface

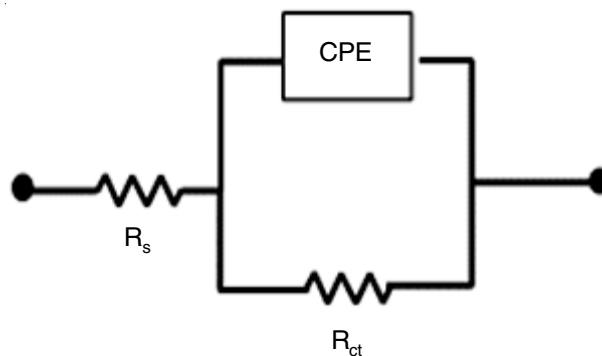


Fig. 7. Equivalence circuit

roughness and inhomogeneity of the metal surface. Therefore, CPE is introduced instead of an ideal capacitor and the effective double layer values C_{dl} is obtained from the following eqn. 7:

$$C_{dl} = (Y_0 R_p^{1-n})^{1/n} \quad (7)$$

A Tafel plot obtained for mild steel in 1 M HCl in the absence and presence of the inhibitor at varying concentrations is shown in Fig. 8. The polarization parameters namely E_{corr} , I_{corr} , anodic slope β_a and cathodic slope β_c , linear polarization resistance LPR values and the IE% calculated from I_{corr} and LPR values are listed in Table-5. The I_{corr} values are found to decrease with the increase in the concentration of the inhibitor and that reflects the formation of protective film on the metal

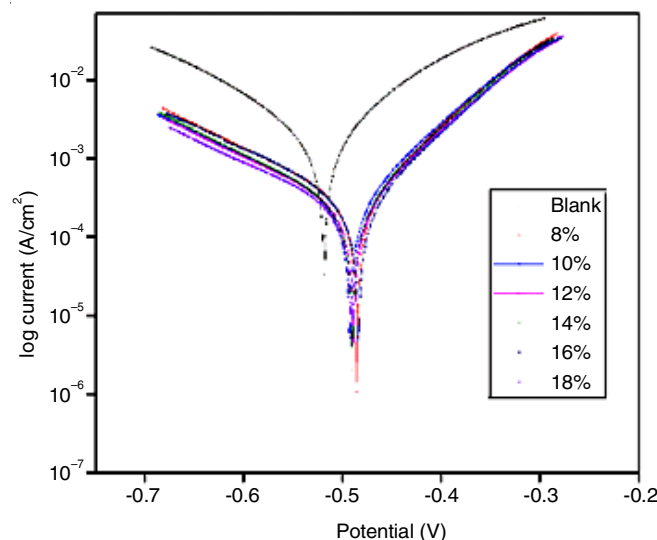


Fig. 8. Polarization curves obtained for mild steel in the absence and presence of lime juice in 1M HCl solution

Conc. (v/v)	Chi-Sq $\times 10^{-2}$	R_s (Ω/cm^2)	CPE* 10^{-4} ($\text{S}^n \Omega^{-1} \text{cm}^{-2}$)	Freq. power 'n'	R_p (Ω/cm^2)	C_{dl} (F cm^{-2})	IE (%)
Blank	2.310	0.8990	1.714	0.8695	25.36	75.8	-
8%	1.830	1.0690	1.629	0.8019	109.9	60.3	76.9
10%	2.869	0.8120	1.594	0.8000	125.1	59.9	79.7
12%	1.371	1.0040	1.368	0.8296	129.0	59.7	80.3
14%	1.640	1.0830	1.326	0.8232	135.9	55.9	81.3
16%	1.840	0.9659	1.297	0.8183	146.3	53.8	82.7
18%	1.740	1.0790	1.163	0.8152	142.8	45.9	82.2

TABLE-5
POLARIZATION PARAMETERS FOR MILD STEEL IN THE ABSENCE AND PRESENCE OF LIME JUICE IN 1M HCl

Conc. (v/v)	E_{corr} (mV/SCE)	I_{corr} ($\mu\text{A}/\text{cm}^2$)	β_c (mV/dec)	β_a (mV/dec)	IE (%)	LPR ($\Omega \text{ cm}^2$)	IE (%)
Blank	-519	1.925×10^{-3}	0.1487	0.118	–	14.9	–
8%	-487	2.993×10^{-4}	0.1616	0.086	84.5	81.5	81.3
10%	-494	2.852×10^{-4}	0.1629	0.088	85.2	87.0	82.8
12%	-489	2.692×10^{-4}	0.1617	0.089	86.0	92.8	83.9
14%	-491	2.709×10^{-4}	0.1626	0.088	85.9	91.7	83.8
16%	-485	2.785×10^{-4}	0.1637	0.091	85.5	91.2	83.7
18%	-491	2.509×10^{-4}	0.1776	0.088	86.9	102.4	85.5



Fig. 9. Optical profilometric 3D images of (a) plain metal (b) metal immersed in blank (c) metal immersed in inhibitor solution

surface. This can be attributed to the blocking of active sites of the metal surface by the inhibitor molecules reducing the corrosion [28]. If the change in the E_{corr} values is greater than 85 mV, the inhibitor can be classified as anodic or cathodic [21,30]. In this experiment, a displacement of E_{corr} is less than 34 mV and hence this inhibitor can be referred as mixed type inhibitor (*i.e.*) can inhibit both anodic dissolution and hydrogen evolution. However, Fig. 8 implies that the inhibitor influences anodic half reaction more than that of cathodic reaction [31].

Optical profilometric studies were performed by the immersion of the mild steel metal in the absence and presence of lime juice in 1 M HCl for an immersion period of 6 h. Fig. 9 display the 3D images obtained for (i) plain metal; (ii) metal immersed in blank; and (iii) metal immersed in 1M HCl containing the optimum concentration of the inhibitor. Table-6 list the values of the surface roughness of the metal samples, which clearly depicts the lowering of the surface roughness of metal samples due to the presence of the inhibitor. This can be related to the decreased corrosion rate in presence of the inhibitor [32].

TABLE-6

OPTICAL PROFILOMETRIC PARAMETERS OBTAINED FOR
a) PLAIN METAL b) METAL IMMERSSED IN BLANK SOLUTION
c) METAL IMMERSSED IN INHIBITOR SOLUTION

Metal samples	Average roughness (S_a)	Root mean square (Sq)
Plain metal	1.062	1.359
Metal immersed in blank	1.541	2.514
Metal immersed in inhibitor	1.154	1.765

Conclusion

The weight loss and the electrochemical studies on the corrosion inhibition behaviour of the acidified lime juice was evaluated for mild steel in 1 M HCl solution. The results showed that lime juice can be used as an efficient corrosion inhibitor for mild steel in acidic medium. Thermodynamic activation

parameters and the corrosion kinetic parameters showed that the inhibition was through a comprehensive adsorption process involving initially a multilayer physisorption followed by chemical adsorption of the inhibitor molecules on the metal surface. Electrochemical studies proved that acidified lime juice is a mixed inhibitor inhibiting both anodic dissolution as well as hydrogen evolution at the cathode. However, from the values of the cathodic and anodic Tafel slopes, it is clear that anodic dissolution is inhibited to a greater extent than that of hydrogen evolution. A decrease in the surface roughness of metal surface when immersed in inhibitor solution can be correlated to the corrosion inhibition efficiency of lime juice.

CONFLICT OF INTEREST

The authors declare that there is no conflict of interests regarding the publication of this article.

REFERENCES

- M. Finsgar and J. Jackson, *Corros. Sci.*, **86**, 17 (2014); <https://doi.org/10.1016/j.corsci.2014.04.044>
- A.S. Yaro, A.A. Khadom and R.K. Wael, *Alexandria Eng. J.*, **52**, 129 (2013); <https://doi.org/10.1016/j.aej.2012.11.001>
- A.S. Yaro, A.A. Khadom and H.F. Ibraheem, *Anti-Corros. Methods Mater.*, **58**, 116 (2011); <https://doi.org/10.1108/00035591111130497>
- Z. Ahmad and F. Patel, *Int. J. Corros.*, **2012**, 982972 (2012); <https://doi.org/10.1155/2012/982972>
- Y. Abboud, O. Tanane, A. El Bouari, R. Salghi, B. Hammouti, A. Chetouani and S. Jodeh, *Corros. Eng. Sci. Technol.*, **51**, 557 (2016); <https://doi.org/10.1179/1743278215Y.0000000058>
- J.C. Da Rocha, J.A.C. Ponciano Gomes, E. D'Elia, A.P. Gil Cruz, L.M.C. Cabral and A.G. Torres, *Int. J. Electrochem. Sci.*, **7**, 11941 (2012).
- X. Wang, Y. Wang, Q. Wang, Y. Wan, X. Huang and C. Jing, *Int. J. Electrochem. Sci.*, **13**, 5228 (2018); <https://doi.org/10.20964/2018.06.36>
- K.H. Rashid and A.A. Khadom, *J. Bio-Tribo-Corrosion*, **6**, 13 (2020); <https://doi.org/10.1007/s40735-019-0312-y>

9. H.D. Ada, S. Altanlar, F. Erdem and G. Bereket, *Int. J. Indus. Chem.*, **7**, 431 (2016); <https://doi.org/10.1007/s40090-016-0077-9>
10. H. Ashassi-sorkhabi, S. Mirzaee, T. Rostamikia and R. Bagheri, *Int. J. Corros.*, **2015**, 197587 (2015); <https://doi.org/10.1155/2015/197587>
11. K.M. Emran, N.M. Ahmed, B.A. Torjoman, A.A. Al-Ahmadi and S.N. Sheekh, *J. Mater. Environ. Sci.*, **5**, 1940 (2014).
12. V. Chinapongtitiwat, S. Jongarootaprangsee, N. Chiewchan and S. Devahastin, *J. Funct. Foods*, **5**, 1151 (2013); <https://doi.org/10.1016/j.jff.2013.03.012>
13. D. Soares, L.M.J. de Carvalho, E.M. Gomes Ribeiro and G.M. Dellamora-Ortiz, ed. B. Valdez, *Food Industrial Process-Methods and Equipment*, Chap. 16, InTech, Croatia (2012).
14. O.K. Buyukkurt, G. Guclu, H. Kelebek and S. Selli, *J. Food Meas. Charact.*, **13**, 3242 (2019); <https://doi.org/10.1007/s11694-019-00246-w>
15. M.S. Waghaye SY Kshirsagar RB and Sawate AR, *Int. J. Chem. Stud.*, **7**, 1098 (2019).
16. F. Khosravi, N. Rastakhiz, B. Iranmanesh and S.S.S. Jafari Olia, *Int. J. Life Sci. (Kathmandu)*, **9**, 41 (2015); <https://doi.org/10.3126/ijls.v9i5.12690>
17. N. Jamil, R. Jabeen, M. Khan, M. Riaz, T. Naeem, A. Khan, N. Us Sabah, S.A. Ghorri, U. Jabeen, Z.A. Bazai, A. Mushtaq, S. Rizwan and S. Fahmid, *Int. J. Basic Appl. Sci.*, **15**, 1 (2015).
18. M.S. Tounsi, W.A. Wannes, I. Ouerghemmi, S. Jegham, Y.B. Njima, G. Hamdaoui, H. Zemni and B. Marzouk, *J. Sci. Food Agric.*, **91**, 142 (2011); <https://doi.org/10.1002/jsfa.4164>
19. E.I. Oikeh, E.S. Omoregie, F.E. Oviasogie and K. Oriakhi, *Food Sci. Nutr.*, **4**, 103 (2016); <https://doi.org/10.1002/fsn3.268>
20. M.H. Othman Ahmed, A.A. Al-Amiery, Y.K. Al-Majedy, A.A.H. Kadhum, A.B. Mohamad and T.S. Gaaz, *Results Phys.*, **8**, 728 (2018); <https://doi.org/10.1016/j.rinp.2017.12.039>
21. A.G. Santos, G.O. da Rocha and J.B. de Andrade, *Sci. Rep.*, **9**, 1 (2019); <https://doi.org/10.1038/s41598-018-37186-2>
22. S. Lahrou, A. Benmoussat, B. Bouras, A. Mansri, L. Tannouga and S. Marzorati, *Appl. Sci.*, **9**, 4684 (2019); <https://doi.org/10.3390/app9214684>
23. R. Karthikaiselvi and S. Subhashini, *J. Assoc. Arab Univ. Basic Appl. Sci.*, **16**, 74 (2014); <https://doi.org/10.1016/j.jaubas.2013.06.002>
24. R.T. Loto and O. Tobilola, *J. King Saud Univ. -Eng. Sci.*, **30**, 384 (2018); <https://doi.org/10.1016/j.jksues.2016.10.001>
25. K. Boumhara, F. Bentiss, M. Tabyaoui, J. Costa, J.M. Desjobert, A. Bellaouchou, A. Guenbour, B. Hammouti and S.S. Al-Deyab, *Int. J. Electrochem. Sci.*, **9**, 1187 (2014).
26. H.A. Emriadi, Yulistia and Velly, *Der Pharma Chem.*, **10**, 79 (2018).
27. U. Nazir, Z. Akhter, N.K. Janjua, M.A. Asghar, S. Kanwal, T.M. Butt, A. Sani, F. Liaqat, R. Hussain and F.U. Shah, *RSC Adv.*, **10**, 7585 (2020); <https://doi.org/10.1039/C9RA10692H>
28. H. Lgaz, S.K. Saha, A. Chaouiki, K.S. Bhat, R. Salghi, Shubhalaxmi, P. Banerjee, I.H. Ali, M.I. Khan and I.-M. Chung, *Constr. Build. Mater.*, **233**, 117320 (2020); <https://doi.org/10.1016/j.conbuildmat.2019.117320>
29. H. Lgaz, S. Masroor, M. Chafiq, M. Damej, A. Brahmia, R. Salghi, M. Benmessaoud, I.H. Ali, M.M. Alghamdi, A. Chaouiki and I.-M. Chung, *Metals*, **10**, 357 (2020); <https://doi.org/10.3390/met10030357>
30. W. Li, *Int. J. Electrochem. Sci.*, **15**, 722 (2020); <https://doi.org/10.20964/2020.01.63>
31. S. Dahiya, P. Pahuja, H. Lgaz, I.-M. Chung and S. Lata, *J. Adhes. Sci. Technol.*, **33**, 1066 (2019); <https://doi.org/10.1080/01694243.2019.1576353>
32. M.H. Sliem, M. Afifi, A.B. Radwan, E.M. Fayyad, M.F. Shibl, F.E.T. Heakal and A.M. Abdullah, *Sci. Rep.*, **9**, 2319 (2019); <https://doi.org/10.1038/s41598-018-37254-7>